Double-Sided Incremental Forming: A Review

Wenxuan Peng
Department of Mechanical, Materials and Manufacturing Engineering,
University of Nottingham,
NG7 2RD, UK
e-mail: wenxuan.peng@nottingham.ac.uk

Hengan Ou[1]
Department of Mechanical, Materials and Manufacturing Engineering,
University of Nottingham,
NG7 2RD, UK
e-mail: h.ou@nottingham.ac.uk

Adib Becker
Department of Mechanical, Materials and Manufacturing Engineering,
University of Nottingham,
NG7 2RD, UK
e-mail: a.a.becker@nottingham.ac.uk

Incremental sheet-forming (ISF) processes have been developed rapidly in the past two decades. Its high flexibility and easy operability have a significant appeal for industrial applications, and substantial progress has been made in fundamental understanding and demonstration of practical implementation. However, there are a number of obstacles including achievable accuracy and instability in material deformation, which are considered as a main contributing factor for preventing the ISF process to be widely used in industry. As a variant of the general ISF process, double-sided incremental forming (DSIF) uses an additional supporting tool in the opposite side of the workpiece, maintains the flexibility, and at the same time improves the material deformation stability and reduces material thinning. In recent years, there has been increased research interest in looking into DSIF-specific material deformation mechanisms and investigation. This paper aims to provide a technical review of the DSIF process as benchmarked with single-point incremental forming (SPIF). It starts with a brief overview of the current state of the art of both SPIF and DSIF. This is followed by a comparative study between SPIF and DSIF with the key research challenges identified. This leads to a recommendation of future directions for DSIF focused research. [DOI: 10.1115/1.4043173]

Keywords: single-point incremental forming (SPIF), double-sided incremental forming (DSIF), formability, toolpath, deformation mechanism

1 Introduction

1.1 Incremental Sheet Forming. Incremental forming may be referred to a number of sheet- and bulk-forming processes such as spinning or rolling that enable workpiece deformation in a gradual or incremental manner. Incremental sheet forming (ISF), also known as single-point incremental forming (SPIF) initially reported by Emmens et al. [1] and Mason and Appleton in 1984 [2], is specifically designated to processes that use particular tools, driven by CNC machines or industrial robots, moving along a predefined tool path to form a clamped metal sheet into the desired shape. Figure 1 shows a schematic of the ISF process, indicating three key elements, i.e., (i) a simple hemispherical forming tool; (ii) blank holder, and (iii) backing plate and partial die [3]. The sheet is clamped on the periphery and the trajectory of the tool is combined by a succession of spiral contours, which determines the geometry and accuracy of the formed products. The main advantages of ISF include its "dieless" feature, easy adaptation, and simple structure of the tool system as compared with many conventional sheet-forming processes, which require a complex press and dedicated tool system. The flexibility and low setup cost allow ISF to be implemented to manufacture low-volume, high-value, and even customized parts [4]. For instance, a limited number of replacement parts have been made by Honda with Amino through the ISF process [1]. Nevertheless, the ISF technology is generally considered to have considerable potential in aerospace, automotive, medical, and other industrial fields.

In recent years, many variants such as two-point incremental forming (TPIF) and double-sided incremental forming (DSIF) have been proposed. As shown in Fig. 2, the classification of the variants of ISF processes is based on the method of applying a supporting tool. The SPIF uses only one tool traveling along a predefined toolpath on one side of the forming sheet, while TPIF uses an extra full or partial die on the other side of the workpiece to increase forming stability. The DSIF process replaces the die with a flexible supporting tool with a specified trajectory.

1.2 Double-Sided Incremental Forming. DSIF was initially studied by Maidagan et al. [5] and Meier et al. in 2007 [6]. It aims to apply a backup force for the better control of the localized deformation and improvement of the formability and accuracy. In the DSIF process, the tool on the top side of the workpiece is generally named as the master tool mainly generating localized deformation, while the tool on the bottom side is named as the supporting tool or slave tool offering a supporting force. The toolpath of the supporting tool is derived from the trajectory of the top tool incorporated with the wall angle and thickness at the contact point. In DSIF, two variants can be classified by the tool moving direction in the radial orientation, i.e., conventional DSIF with the out-to-in toolpath (Fig. 3(*a*)) and accumulative double-sided incremental forming (ADSIF) with the in-to-out toolpath (Fig. 3(*b*)). In the conventional DSIF process, the tools move continuously from the maximum fringe of the workpiece toward the center. The tool steps along the negative Z direction with an incremental depth ΔZ and forms the material in the horizontal X–Y plane at the current Z depth. In ADSIF, the tools start from the minimum annulus of the clamped sheet and simultaneously move down by an incremental depth ΔZ. Then, both the master and slave tools travel on the X–Y plane while keeping at a constant $Z = -\Delta Z$. Generally, ADSIF is regarded as a specific toolpath strategy of DSIF. However, it is worthwhile to discuss and compare ADSIF with SPIF and DSIF due to its enhanced formability, accuracy, and unique deformation mechanism [7].

Consequently, the purpose of this review is to introduce the current development of DSIF, including comparison with SPIF in terms of toolpath design, formability, and material deformation mechanisms. This is followed by the identified research gaps in the field of DSIF and recommendations for further research.

2 Comparison Between SPIF and DSIF

As a mainstream in the ISF field, extensive studies have been carried out on the aspects of SPIF concerning accuracy, toolpath strategy, deformation, and failure mechanisms. There are many published reviews of SPIF that concentrate on its history, the improvements, and limitations compared with the conventional sheet-forming processes, also the deformation and failure mechanisms [1,8–11]. The advantages of SPIF include high flexibility,

[1]Corresponding author.

Manuscript received March 12, 2018; final manuscript received December 12, 2018; published online March 27, 2019. Assoc. Editor: Gracious Ngaile.

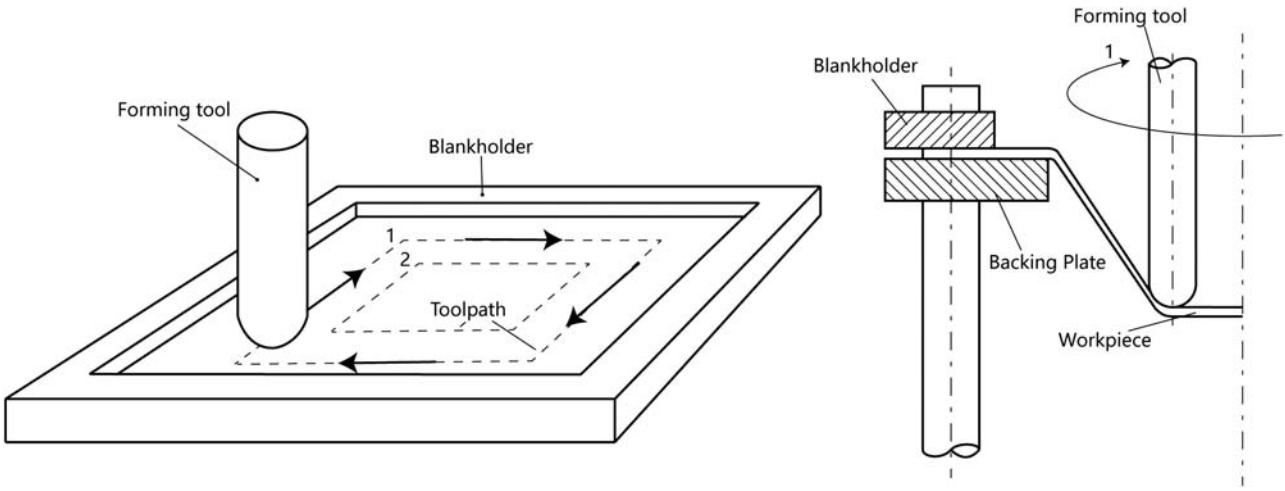

Fig. 1 Illustration of incremental sheet forming (reproduced from Ref. [1] with permission from Elsevier © 2010)

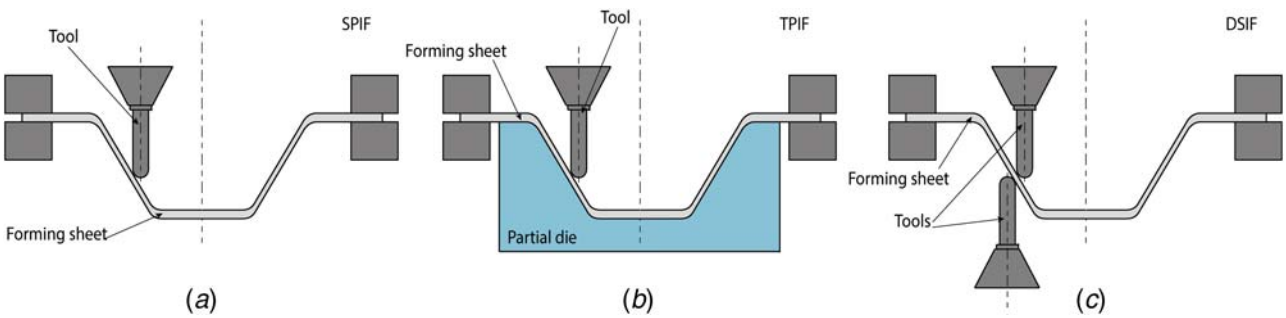

Fig. 2 Schematics of (*a*) SPIF, (*b*) TPIF, and (*c*) DSIF

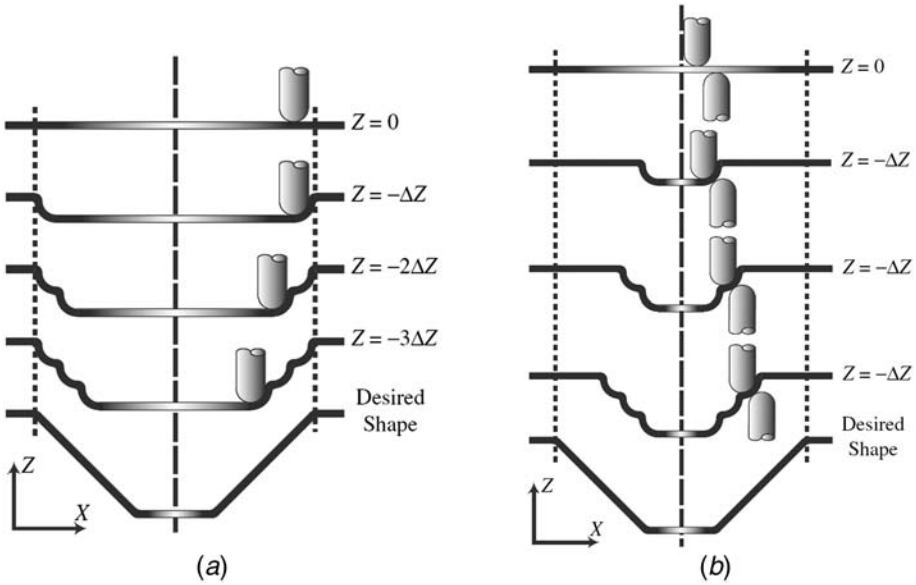

Fig. 3 Schematics of (*a*) conventional DSIF toolpath and (*b*) accumulative DSIF toolpath [7] (reprinted with permission from Springer © 2013)

low setup cost, and improved formability [8,9]. However, the SPIF process is also limited by the slow-forming speed, insufficient accuracy, rough surface finishing, and small achievable wall angle [9]. A number of reviews focus on specific aspects of ISF processes such as the effects of the process parameters [12], hardware [13], asymmetric incremental sheet forming [14], toolpath strategies [15], and FEA research [11]. Future prospects were also suggested in terms of the mechanism studies, prediction by FE simulations, and the extension of small-scale production and industrial applications [11].

While notable advances have been made in SPIF processes, specific limitations of SPIF have also been identified by various studies through experimental testing or theoretical analysis. The localized deformation under ISF process results in the high dependence of

the geometrical accuracy on the stability of the deformation occurring around the contact region [16]. The springback effect and the artificial dynamic oscillations in contact area are also reported as the main resource of error [7,8]. The optimization of toolpath and the application of the supporting tool are commonly used to overcome the drawbacks of SPIF. In terms of the optimization of toolpath, the starting point, direction of tool movement, and the distance between two adjacent contour lines are optimized and tested to be effective [17,18]. Techniques like FEA and closed-loop feedback control system are combined with the toolpath design and successfully enhance the geometrical accuracy and homogeneity of the parts produced [19,20]. In terms of the additional support, the TPIF process has been proven that the partial die helps to reduce the springback upon the unloading in SPIF, and thereby the formability and accuracy are improved [3,21,22].

DSIF also brings comparative benefits by using an additional tool support, instead of the partial die in the TPIF process, to achieve improved formability and accuracy to the SPIF process. DSIF was studied by Meier et al. [6] as a truly "die-less" TPIF method and was tested and compared with SPIF through a robotic system. A simply truncated cone was produced separately by SPIF and DSIF processes. The thickness deviation results show that the cone fabricated by DSIF has more homogeneous error dispersion than using SPIF. According to the comparison between SPIF and DSIF from published papers [23,24], the additional supporting tool can effectively reduce the geometrical deviation. The die-less feature makes DSIF an economical solution to resolve the current problems in SPIF.

A full comparative investigation using both experiment and FE simulation was conducted by Lasunon and Knight [25] looking into the stress and strain condition, thickness, and part profile. A shallow square-sided pyramid with 38 mm dimension for open width, 4.6 mm for depth was chosen as the desired shape in both experimental and analytical trials. The material was AA5052 alloy and two-wall angles were tested to evaluate the performance of both processes to the distinct angles. It was observed from contour plots (Figs. 4(*a*) and 4(*b*)) that the peak value of equivalent strain in SPIF was higher than that of DSIF when forming the same shape; on the aspect of thickness (Figs. 4(*c*) and 4(*d*)), the sheet thinning from SPIF process was greater than that by DSIF, and the thinning concentrates in the corner in SPIF when it happened in the wall area in DSIF [25]. Therefore, the failure is more likely to occur in the wall region in DSIF instead of the corners from SPIF. The contrast of minimum thickness values indicates an advantage of DSIF process that can be utilized to produce parts with sharper edges and steeper wall angle as compared with the SPIF process.

The deformation instability, which limits the accuracy and formability of the SPIF process is improved by the implementation of the support tool in DSIF. However, the support tool was found to lose contact with the workpiece at an early stage of the process in both experimental test and FE simulation conducted by Maidagan et al. [5], suggesting the process degenerated to SPIF. This fact confirms that the control of the support tool to avoid loss of contact due to the unexpected material thinning is a key challenge in DSIF research. Thus, the prediction of sheet thickness distribution is an important question to maintain the improved formability in DSIF, which is very different from the SPIF process.

In both SPIF and DSIF processes, the sheet is clamped and formed by the movement of specific tools. Most of the advantages of SPIF are inherited by DSIF, such as high flexibility and no requirement of dies. DSIF shows the potential to surmount the formability limits and low geometric accuracy in SPIF [25,26]. The value of plastic strains and the extent of sheet thinning concentration in SPIF are higher than that in DSIF, which means that the possibility of failure occurrence in DSIF is less than that of SPIF. Therefore, the aforementioned studies show a clear advantage of the DSIF over SPIF in a number of key attributes under general ISF-processing conditions.

3 Formability in DSIF

3.1 Definition. The formability in the sheet-forming process is used to describe the ability to enable sheet deformation without material failure. Similar to the SPIF process, the formability of

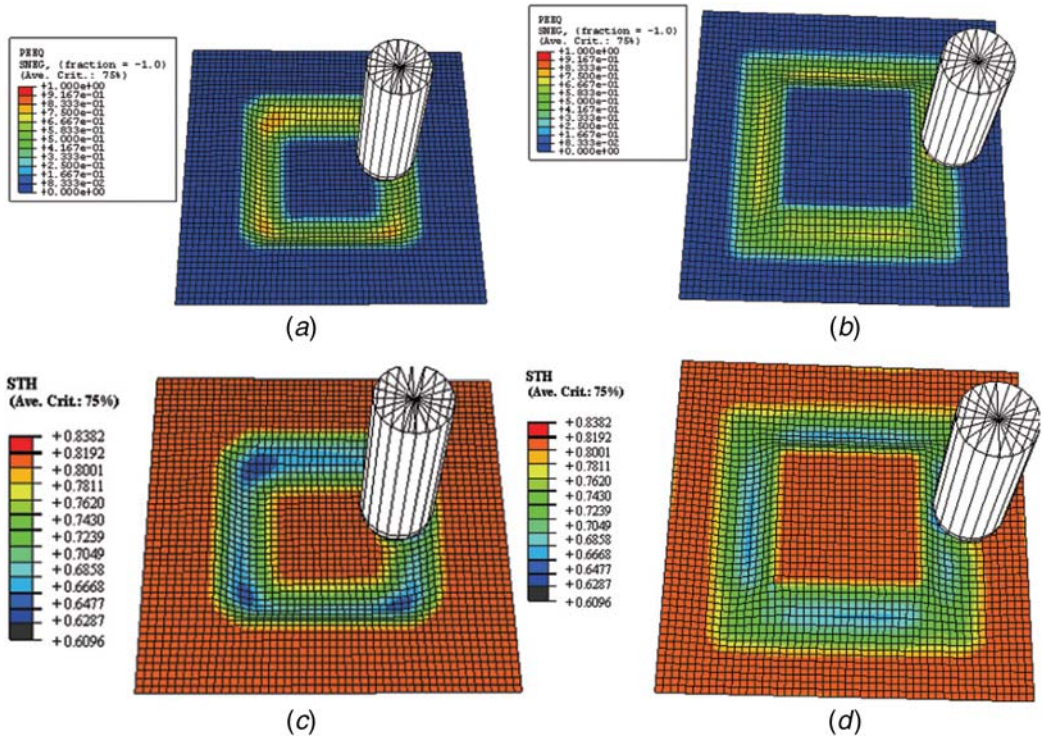

Fig. 4 Equivalent plastic strain contour plot of (*a*) SPIF and (*b*) DSIF; thickness distribution in (c) SPIF and (*d*) DSIF process of 45 deg pyramids [25] (reprinted with permission from SAGE © 2007)

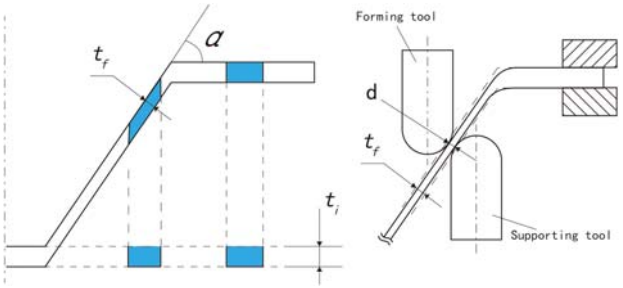

Fig. 5 An illustration of the sin law and squeeze factor in DSIF

DSIF can be described by the maximum achievable wall angle α_{max} according to the sine law as shown in Eq. (1).

$$t_f = t_i \sin(90 \text{ deg} - \alpha) \tag{1}$$

where t_f and t_i are the final and initial wall thickness, respectively, and α is the wall angle (Fig. 5) [27]. Using the sine law, the wall thickness can be uniquely determined by the wall angle α. Considering the potential squeezing effect brought by the support tool, another parameter called squeeze factor s, suggested by Malhotra et al. [23], was used to estimate the extent of an artificial squeezing effect applied on the thickness in the contact region as defined in Eq. (2), where d is the current thickness of squeezed wall:

$$d = s \cdot t_f \tag{2}$$

The squeeze factor s demonstrates the ratio of the final formed thickness to the thickness predicted by the sine law. It has various influences but cannot indicate to formability of the processes. According to the sine law, the sheet thickness decreases and the chance of failure rises when the wall angle increases. Thus, the maximum achievable wall angle α_{max} is regarded as the most important indicator for the formability of the DSIF process and has been widely implemented in a comparative study [24] and a parametric investigation [28,29].

The indicators of formability in ISF can also be used in DSIF, especially for analytical studies. Lu et al. [30] used the stress triaxiality, which is previously used to evaluate the contribution of deformation mode combined with stretching, squeezing, and shearing in the ISF processes, as an indicator of the enhanced formability of the DSIF process. Based on the traditional forming limit diagram (FLD) [10], Allwood and Shouler [31] proposed a generalized forming limit diagram (GFLD), which took the normal stresses and through-thickness shear into consideration to match the nature of the deformation mechanisms of DISF. The general methods for the evaluation of process formability can be used to support the analytical research of DSIF [7], although a specific procedure or approach for adaptation and implementation is still to be fully researched and validated.

3.2 Influential Factors in the Formability of DSIF. The DSIF process inherits the localized deformation feature of the general ISF processes and hence the dependence of formability on process parameters such as tool rotations, feed rate, and step size [12]. However, the use of the support tool and its interactions with the workpiece and the master tool requires further research to the formability of the DSIF process. Lu et al. [30] implemented a series of experiments with dedicated support tool mounted on a pneumatic actuator in order to investigate the effect of tool shift and compressive stress in DSIF. The effect of tool shift and compression were estimated via checking the deformation of predrilled holes in the through-thickness direction (Fig. 6). Based on the observation of results, the stretching in meridional direction is considered to have a dominant effect in the deformation of DSIF. The other factors are the compression in the radial direction and slight through-thickness shear in the tool movement direction. The compressive stress shows a positive effect on the formability. However, excessive supporting forces generating too much squeezing pressure reduce the formability in DSIF. Similarly, the tool shift has a positive effect on the enhancement of formability and would change the position of fracture occurrence. This approach was successfully used to form pure titanium cranioplasty plate for medical applications [32].

Ren et al. [28] processed a parametric study using FE simulation to investigate the influential factors on formability in the ADSIF process. As shown in Fig. 7(*a*), the tool gap T_g and the position angle θ were chosen as the variables, and the stable wall angle was measured as the criterion of formability (Fig. 7(*b*)). It is found that the dominant influential factor is switched between T_g and θ depending on the extent of the squeeze effect. When squeezing is the dominant deformation mode during the process ($T_g \leq 0.7$), T_g has the leading effect on the stable angle; when bending is the main deformation mode ($T_g \geq 1$), θ is the dominant factor instead of T_g; when the process is in the competing region ($0.7 < T_g < 1$), there are implicit

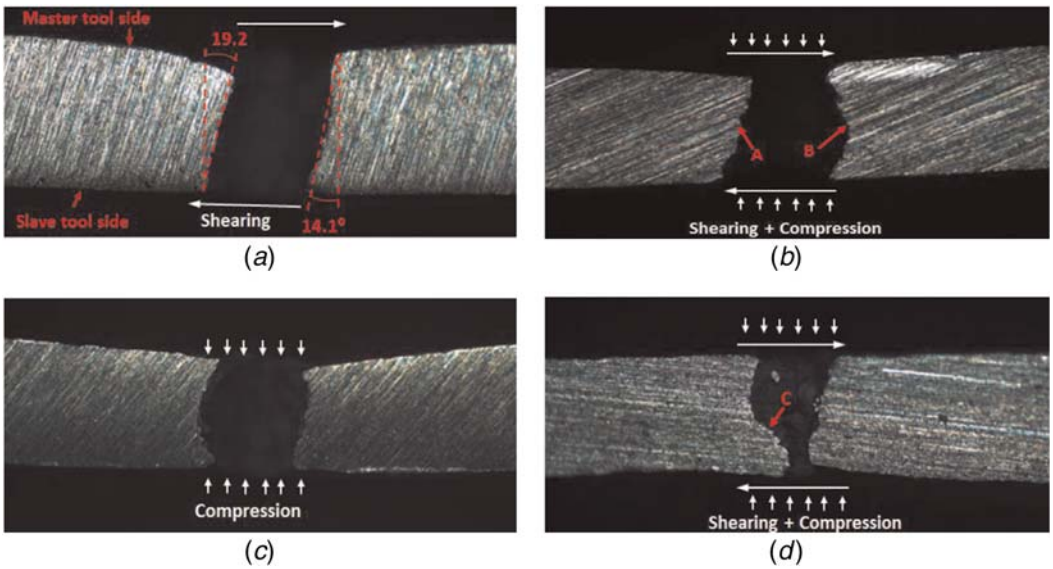

Fig. 6 Material deformation via different supporting forces and tool shift: (*a*) 240 N without tool shift, (*b*) 240 N with tool shift, (*c*) 480 N without tool shift, and (*d*) 480 N with tool shift [30] (reprinted with permission from Elsevier © 2015)

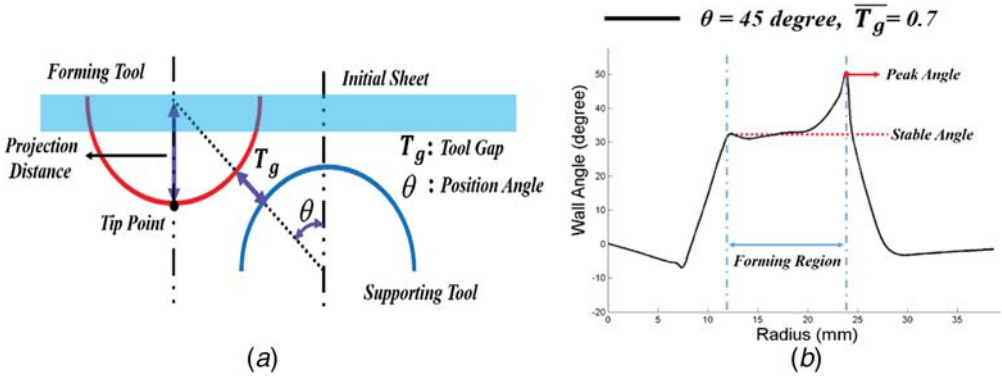

Fig. 7 (*a*) Schematic of toolpath variables and (*b*) definition of stable angle [28] (reprinted with permission from ASME © 2015)

influential factors of process formability. This result may be partially explained by the force transfer due to the changes of T_g. When $T_g < 1$, the forming force increases dramatically with the T_g decreasing. Also, θ affects the bending instead of squeezing and makes the transition from the current wall angle into a stable wall angle. Therefore, keeping the process under the competing or bending-dominant region ($T_g > 0.7$) and increasing the position angle θ is recommended to control the squeezing effect, as well as the forming force, in an appropriate range to reach the maximum formability in ADSIF forming. However, this conclusion may not be applicable to the conventional DSIF process due to significant differences between the ADSIF and DSIF processes, which are discussed in Sec. 5 on deformation mechanisms.

3.3 Electrical-Assisted Heating in DSIF. Several trials were reported for various materials being tested in ISF including composite and high-strength materials. Preliminary studies for composite materials focused on the formability and failure mechanics of polymers [33] or metal-polymer/foam/fiber [34–36] by the SPIF process. Davarpanah et al. [37] presented a series of experiments for thermoplastics using SPIF, conversational DSIF and ADSIF processes to give a comprehensive assessment. The results showed an agreement with previous tests using a metal sheet that the DSIF process postpones or avoids the occurrence of fracture on the polymer sheet as well. The scanning electron microscopy (SEM) images demonstrated less void growth in the parts of polymer made by DSIF, which leads to a discussion that the heat generated by the additional tool due to frictional heat effect causes the formability improvement, instead of the compression effect when forming sheet metals.

For hard-to-form materials, heating is a generally used solution to increase the formability of materials in the ISF processes. There are various methods developed for heating-assisted ISF including mounting heating equipment (e.g., hot air blowers [38], heater band [39], and laser generator [40]), friction stir heat [41,42], and electric heating [43,44]. Xu et al. [45] investigated electrically assisted DSIF in forming an AZ31B magnesium alloy. Two modes of electrical connection were discussed (Fig. 8(*a*)). An air cylinder and rolling-ball tool were used to eliminate loss of contact and electrical discharging phenomenon. In contrast to the electrical SPIF process, the formability, geometric accuracy, and surface finishing were improved (Fig. 8(*b*)). Valoppi et al. [46] conducted an electrically assisted ADSIF process to form a Ti6Al4V alloy. The electric current was applied directly to two forming tools and the value of electric current was the main variable to control the temperature during the process. In the results, the formability improvement was apparent as almost all specimens fabricated with the electrically assisted ADSIF could achieve a larger depth than the normal ADSIF process without cracks. However, the best-achieved depth was obtained in the 50 A case. Then, the negative effect appeared when the applied current value increased above 50 A. The reason could be the decrease of forming force and the release of the internal stresses due to the thermal effects during the process. A specific advantage of heat-assisted DSIF over SPIF is potentially the local heating effect by tool rotation friction or direct resistance heating from both sides of the workpiece to allow more even heating and greater controllability under ISF deformation conditions.

4 Toolpath Design in DSIF

Toolpath design and optimization are the mainstreams of DSIF research. The key questions to be solved through toolpath design are insufficient geometrical accuracy and loss of contact due to

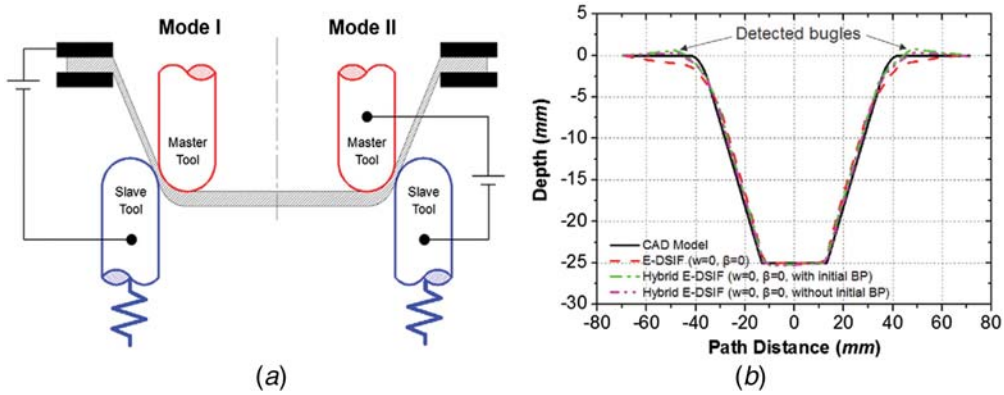

Fig. 8 (*a*) Two electrical connection modes in DSIF and (*b*) improved geometry accuracy in electrically assisted DSIF [45] (reprinted with permission from Elsevier © 2016)

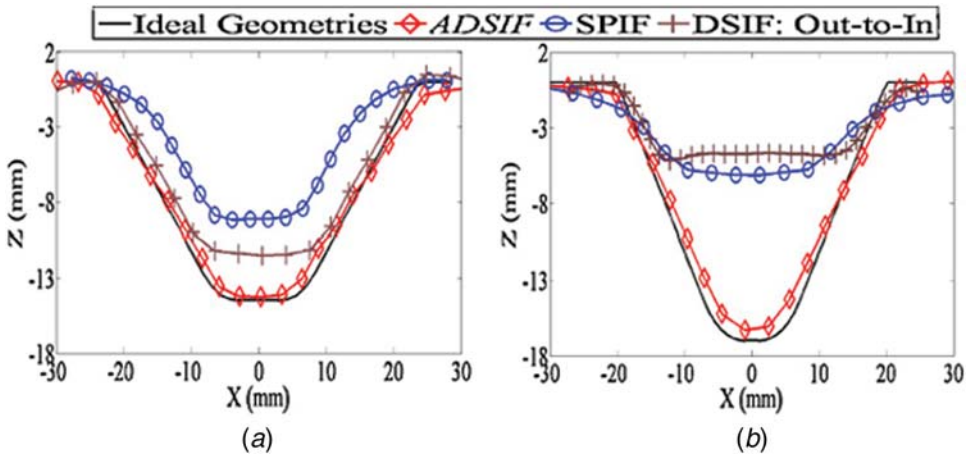

Fig. 9 Comparison of geometries of components made by ADSIF, DSIF, and SPIF with wall angles (*a*) 40 deg and (*b*) 50 deg [24] (reprinted with permission from Elsevier © 2012)

the unpredictable material thinning. The basic principle of toolpath design is the sine law, which is consistent with conventional ISF. The toolpaths can be classified into two options: traditional out-to-in DSIF and in-to-out ADSIF strategies. Several prediction and compensation strategies are applied based on DSIF and ADSIF processes. The advantages and limitations of each strategy are discussed.

4.1 Accumulative-DSIF Strategy. ADSIF requires a novel toolpath that uses two tools forming the sheet via an initially single incremental depth and horizontal in-plane motion. ADSIF has two main differences from the conventional DSIF strategy: (i) the tools are moving from minimum annulus to the fringe and (ii) after the first step, tools are positioned at the $Z=-\Delta Z$ level without any movement in vertical axis throughout the process. A significant advantage of ADSIF is that two tools maintain contact with the forming sheet and mechanically avoid the loss of contact throughout the whole process.

The constant contact leads to the improved formability and geometrical accuracy in the ADSIF process as compared with the conventional DSIF and SPIF processes [47]. The ADSIF concept was originally introduced and tested by Malhotra et al. [24]. Two cones with wall angles of 40 deg and 50 deg were formed to test the forming limit and precision with the reference parts made by SPIF and DSIF for comparison. As a result, the smaller geometric deviations and thickness inconsistency were observed from parts produced by ADSIF instead of SPIF or conventional DSIF (Fig. 9). When forming a cone with 50 deg draw angle, fracture occurs in the processes except ADSIF (Fig. 9). On the other hand, a small incremental depth is required in the ADSIF process to sustain the high accuracy and results in considerable time for completion. Additionally, the achievable wall angle is hard to exceed much more than 50 deg [48].

Although the long forming time and the limitation of forming wall angles in ADSIF prevent it to be a full replacement of conventional DSIF, the improved formability and quality by ADSIF still attract attention for further studies. Toolpath optimization and combination with out-to-in DSIF toolpath are verified to be beneficial for the enhancement of formability and profile accuracy [47]. Other numerical analyses reveal the unique deformation mechanism in ADSIF of enhanced shearing and bending effect in contrast to dominant stretching and bending effect in conventional DSIF processes [7,29]. In summary, the ADSIF is a noteworthy strategy and has a considerable potential of applications.

4.2 Compensation-Based Toolpath. Toolpath compensation is one strategy to accurately predict the deflection during the process and counteract the springback effect through the optimization of tools trajectory. Meier et al. [49] presented experiments of model-based and sensor-based strategies in robotic forming. An adjustment vector, derived from the deviation obtained by simulation results and CAD model (Fig. 10), was defined as a key parameter for toolpath revision. In terms of the sensor-based method, actual geometry is obtained through a 3D surface scanner and projected onto the reference CAD model in the direction of the adjustment vector with the aim of plotting counter points of the next forming run. For the model-based strategy, the process is simulated through an FE model with adjustment made based on the geometric errors obtained from the simulation result. Both strategies were verified to be able to reduce the deviations with results showing a significant reduction of deviation from ± 1 mm to ± 0.25 mm using the sensor-based strategy, and 0.7 mm in z-direction with 1 mm in the y-direction using the model-based strategy. To improve the performance of the model-based approach, the springback effect should be taken into account in the FE model.

Rakesh et al. [50] developed another toolpath strategy that takes the deformation of tools into consideration. The adjustment vector was made up by sheet and tool deflection separately calculated by the predicted forming forces (Fig. 11(*a*)). The geometry obtained in the first iteration of FE simulation was compared with the desired shape to predict the deflections and to generate the compensated toolpath (Fig. 11(*b*)). In order to optimize the forming process of varying wall angle or asymmetric component, the desired profile was divided by geometric features to predict forming forces more precisely (Fig. 11(*c*)). Based on the results of several tests with different shapes and features, it can be confirmed that

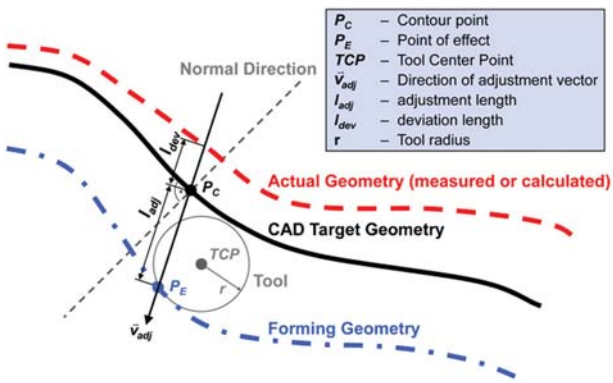

Fig. 10 Schematic of applying the correction through the reference CAD model [49] (reprinted with permission from Springer © 2013)

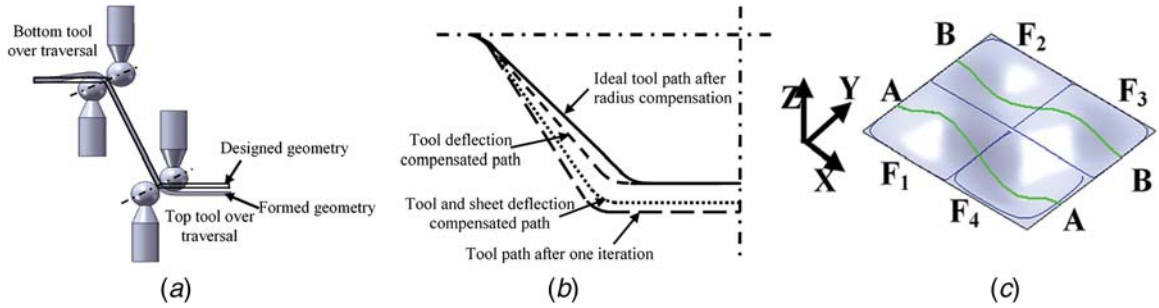

Fig. 11 (*a*) Toolpath and sheet deflection, (*b*) steps of how compensation applied, and (c) partition of profile based on features [50] (reprinted with permission from ASME © 2016)

the deflection-compensated toolpath strategy can enhance the geometrical accuracy of DSIF as the measured maximum error is less than 0.5 mm. The maximum deviation can maintain under 0.6 mm in the fringe region after component being trimmed.

Another approach to compensate for tool deflection was proposed by Ren et al. [51], who developed a closed-loop algorithm to eliminate the inaccuracy from the tool deformation and the system error from motor drivers or controllers. A model coupled with the stiffness of the forming tools, machine, and the sheet metal under squeezing was established to derive the system response from force to displacement. Therefore, the loss of contact can be avoided, and the state of stresses is under control by monitoring the reaction force on the supporting tool. In the tests, the produced asymmetric and complex parts proved the effectiveness of this algorithm toward maintaining the contact between tools and sheet as well as the enhancement on the formability and geometric accuracy.

Wang et al. [52] proposed a novel strategy to reduce the springback in the DSIF process with a dedicated pneumatic supporting tool. The position between the master and slave tools was relatively rotated as shown in Fig. 12. With the constant supporting force, the "reverse-bending" or "squeezing" effect can be produced in the local forming region according to the rotation angle. The error in both major and minor axis on the semi-ellipsoid cone part was measured and compared to demonstrate the restraint effort from different strategies to the springback effect. The numerical and experimental results showed an agreement that both the squeezing and reverse-bending strategies can reduce the offset due to springback effect, while the reverse-bending strategy can achieve more accurate geometry than the squeezing strategy.

Comparing the compensation strategies conducted by Rakesh et al. [50] and Meier et al. [53], the method considering the compensations of both sheet and tools shows advantages of higher accuracy and the capability of adaption for complex features. This may be attributed to the accurate force prediction (within 50 N of deviation compared with the experimentally measured forming forces) and reasonable arrangement of toolpaths. Simplified algorithms with the consideration of tool machine stiffness [51] and "squeezing" and "reverse-bending" strategies [52] can be implemented in DSIF processes for improved accuracy and inhibition of the springback without requiring for predicted forming forces or deflections.

4.3 Feature-Based Toolpath Strategy. The feature-based approach was initially proposed by Lu et al. [18] for SPIF that was based on the local characteristics of profile and design-specific toolpath with the aim of enhancing the accuracy. The final toolpath utilizes an interpolation technique from Malhotra et al. [54]. This strategy was further developed to be adaptive to the DSIF process by Lingam et al. [55] and Ndip-Agbor et al. [56]. The additional support tool provides the suitability for more forming features and sequences. The initial step is the establishment of the component model and reading features from the desired surfaces to generate silhouettes. These silhouettes or saddle points are matched to the

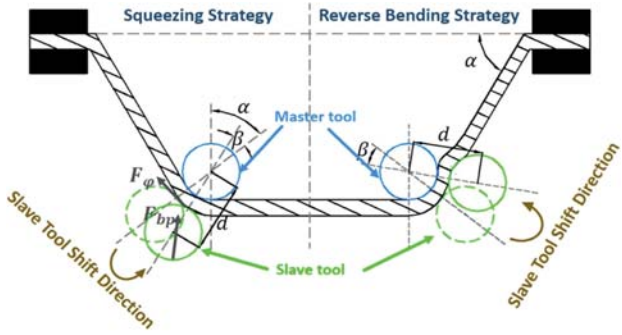

Fig. 12 Illustration of squeezing and reverse-bending strategies for anti-springback purpose [52] (reprinted with permission from Springer © 2018)

characteristics of features to recognize the geometrical features correctly. Then, a proper forming sequence of features is selected in checking the corresponding effects between adjacent feature forming steps and the algorithm calculates the rectifying parameters. Finally, the DSIF toolpath is generated using helical trajectory incorporating deflection compensation.

Improvements in surface finish, geometric features, and accuracy were confirmed by experiments. Maximum deviation to the ideal profile can be controlled under 0.4 mm when the correct forming sequence and strategy were applied. Moser et al. [57] developed another analogous method corresponding to the in-plane curvature effect. It was observed that the region of loss of contact was affected by the tool motion direction (Fig. 13(*a*)). The forming force on the slave tool in the *Z*-direction also shows a drop after forming a turning point at the corner that indicates the occurrence of loss of contact (Fig. 13(*a*)). The toolpath was divided into four parts according to the contour protrusion and tool moving direction (Fig. 13(*b*)). Then, the compensation was applied to the region with insufficient support. As a result, the uniformity of thickness distribution was improved and the possibility of failure was reduced.

Zhang et al. [47] proposed a mixed strategy that combined DSIF and ADSIF methods. ADSIF was used to form the main body of the part to avoid the 0loss of contact and to achieve a better geometry, whereas DSIF was used to form the finer details on the part in the next step. As a result, the mixed strategy can form the part with larger forming depth than that implemented by only using the conventional DSIF process and achieve better details than that obtained from only the ADSIF method (Fig. 14). However, it was also found that the fracture occurred during the DSIF process when forming parts of a large wall angle. The forming limits of both the DSIF and the ADSIF need to be investigated for further development of combined forming strategies.

In conclusion, the feature-based strategy is a useful method to optimize the toolpath with different geometrical features. The feature-based strategy can be generalized in the form of detailed guidelines of toolpath design in the DSIF process, similar to the

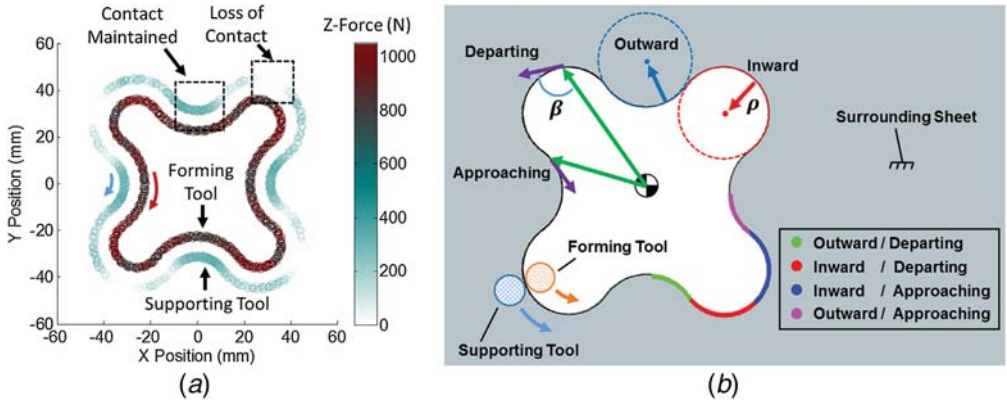

Fig. 13 (*a*) Contour plot of *Z*-forces predicted via FE simulation and (*b*) classification of tool movement based on tool movement and contour [57] (reprinted with permission from Elsevier © 2016)

study presented in SPIF [15]. Two essential issues to be addressed are the separation of the contour model and the implementation of compensation. The feature-based and compensation-based strategies are compatible with each other and can be incorporated together for further enhancement of formability and accuracy, which is considered as a main research direction for the DSIF toolpath optimization. There is a clear need for further study on the precision of feature recognition and corresponding optimization methods.

5 Deformation Mechanisms of DISF

The deformation modes and fracture mechanisms are important research topics in the ISF field. The deformation mechanisms in SPIF are generally the combinations of bending, stretching, and shearing depending on the forming conditions [31]. An appreciable amount of studies also focuses on the local deformation around the contact point and concludes the significance of the plain strain stretching, bending-under-tension (BUT), and through-thickness shear to the improvement of material formability [10,58–60]. In this area, FEA helps to gain in-depth understanding of the strain and stress development as well as the fracture. On the other hand, many damage models have been developed based on classic fracture theories, including Gurson–Tvergaard–Needleman model and Lemaitre continuum damage mechanics model to provide an insight in fracture mechanisms [61–64]. Similar studies are making progress in the DSIF field based on the methods such as FEA [7], parametric research [28,29], or the stress analysis amended from the previous SPIF studies [30]. The clear understanding for the deformation mechanisms in various ISF processes helps to learn the reasons for the disparities and the ways for further improvement of formability and geometry accuracy in SPIF, DSIF, and ADSIF [30].

5.1 Deformation Mechanisms in DSIF. The deformation mechanisms in DSIF have been discussed in early comparative studies between SPIF and DSIF and toolpath research. A significant difference being revealed by FE method is that the maximum equivalent plastic strain in the DSIF process is less than that in SPIF and the failure caused by material over-thinning is more likely to occur in the wall region in DSIF, while it happens more in the corners in SPIF [25]. Malhotra et al. [23] found that the squeezing effect of tools leads to the higher plastic strains concentrating in a small area around the contact point of the tools and workpiece. In experiments, this compressive effect results in high strain hardening of the formed part. This phenomenon was explained by a comprehensive investigation of mechanism in DSIF presented by Lu et al. [30]. Based on the similarity between the deformation mechanics in SPIF and DSIF, a membrane method was implemented in the stress analysis where the shear effect was only considered to occur in the tangential direction. The stress triaxiality was selected as an indicator of formability. As a result, the drop of stress triaxiality with the increase of equivalent strain in DSIF (Fig. 15(*a*)) was found, whereas in SPIF the stress triaxiality underwent a stationary development throughout the process (Fig. 15(*b*)). It was concluded that the drop of stress triaxiality produced by the support tool in DSIF deferred the occurrence of failure and helped achieve a greater wall angle than in SPIF. Compared with the previous mechanism studies in SPIF, the additional squeezing and shear effects were the main differences. However, the distinct effects of compression and shear need to be further investigated.

Valoppi et al. [65] investigated the fracture in the E-DSIF forming process with Ti-6Al-4V sheet. Three electric current intensities (50 A, 87.5 A, and 100 A) were applied on both the master and support tools to investigate the sheet fracture under different temperatures. The E-DSIF process was conducted until the sheet fracture occurred and the fracture surface was checked by using SEM. To investigate the material failure behavior, the SEM results from the tested samples were compared with samples from uniaxial tensile and pure shear tests under corresponding temperature cases. The achievable forming depth was increased with the rise in current intensity. It was observed that the fracture began from the outer surface, then propagated along the tool movement direction and ended when the laceration formed. The fracture can be classified

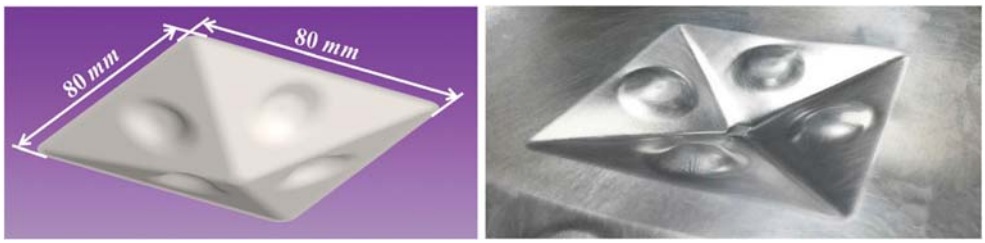

Fig. 14 The desired and final product fabricated via the mixed toolpath strategy [47] (reprinted with permission from ASME © 2015)

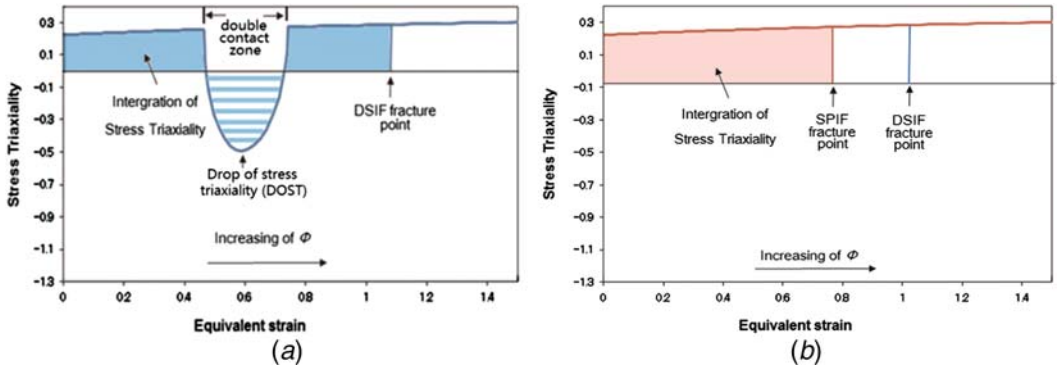

Fig. 15 Comparison plots of equivalent strain versus stress triaxiality in (*a*) DSIF and (*b*) SPIF [30] (reprinted with permission from Elsevier © 2015)

as mode I, also named as tearing by the SEM analysis. Combined with the analysis by Lu et al. [30], the fracture in E-DSIF is more likely to happen in the formed region during the progressive thinning of the sheet, instead of the compressive area contacted with both the forming tool and the supporting tool. The reason can be that the material ductility in the compressive area is increased due to local heating and the compressive pressure, which postpones the fracture because of the drop of stress triaxiality.

5.2 Deformation Mechanisms in ADSIF. ADSIF, as a specific toolpath strategy of DSIF, exhibits a degree of peculiarity and different patterns of deformation mechanisms. This was initially revealed through FEM by Smith et al. [7]. An eight-layer model of linear brick elements with reduced integration is used for both SPIF and ADSIF analysis (Fig. 16(*a*)). A radial mesh strategy was applied in order to capture the material behavior in the directions parallel and perpendicular to the tool movement. Moreover, four sections along the forming depth were created (Fig. 16(*b*)) to investigate the changes of strain components and hydrostatic pressure throughout the forming process. With the comparison of SPIF, a general view of the deformation of ADSIF can be analyzed. In summary, the dominant deformation modes in ADSIF are local bending around the contact point between the tools and forming sheet, combined with a squeezing effect as well as a shear effect perpendicular and parallel to the tool moving direction. In contrast to SPIF, there are significant but consistent differences between the plastic strains as observed on the inner and outer surfaces in ADSIF, which may be attributed to bending and high through-thickness shear effect. The support tool results in increased compressive pressure and shear. Compared with the DSIF process, ADSIF is characterized by high through-thickness shear and the lack of downward pressure because the counteracting effect from material bunching reduces the stretching effect.

Ren et al. [28] presented a parametric study using a simplified FE model to improve the simulation efficiency without losing too much accuracy in wall angle prediction (Fig. 17(*a*)). A clamped narrow strip model was implemented to simulate a part of ADSIF process, which consumed 10–15 min for simulation instead of 7–10 days with a full scale of ADSIF model. The relative tool position, described as the horizontal distance D and vertical distance S, are used as research variables (Fig. 17(*b*)). To compensate for the accuracy loss due to the simplified model, the Latin Hypercube Sampling method is applied to find the relationship between the values of D, S, and the achievable wall angle. The prediction via the simplified model was very close to the experimental results in a certain range of angles and the deviation was controlled within 5 deg. The results show that the combination of the values of D and S is not unique when forming a specific wall angle [29,66]. A similar parametric study was also reported by Ren et al. [28] as the tool gap and tool position angle were chosen as parameters. The stable wall angle in the forming region was used as a representative indicator of the whole formed part. The entire ADSIF model with an advanced mesh density of eight layers of solid elements was executed using LS-DYNA. Thus, the accuracy of FE prediction was significantly improved at the cost of long simulation time. The conclusion agrees with the deduction of Lu et al. [30] that the excessive squeezing brings a negative effect on formability.

6 Discussion and Conclusions

The DSIF process has been shown to be able to achieve improved formability and geometric accuracy as compared with the SPIF process. The additional tool provides extra supporting force and increases the deformation stability while the benefit of high flexibility is kept and the low setup cost feature is maintained as compared with the TPIF process. Most of the published research focus on the

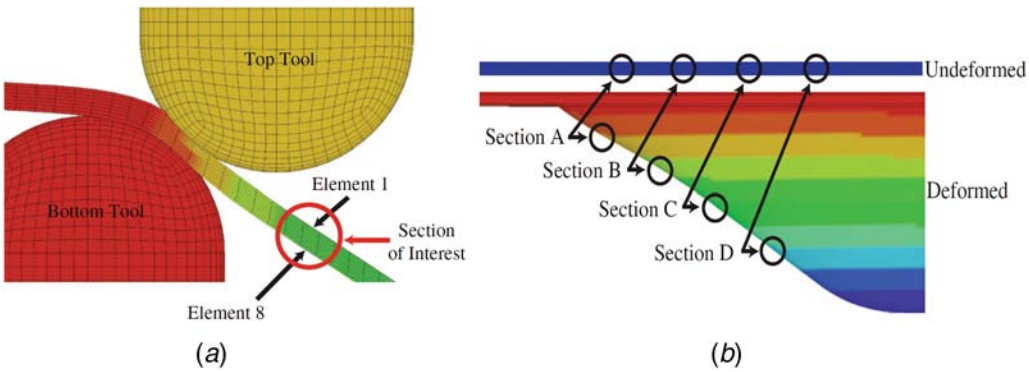

Fig. 16 (*a*) FE model for ADSIF and (*b*) deformation sections for different forming stages [7] (reprinted with permission from Springer © 2013)

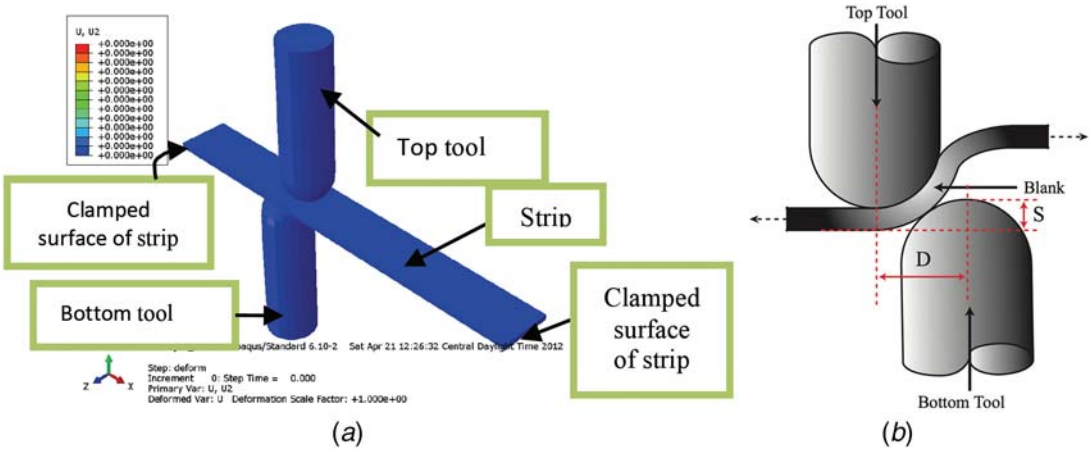

Fig. 17 Schematics of (*a*) simplified ADSIF model and (*b*) variables *D* and *S* in ADSIF [29,66] (reprinted with permission from Springer © 2015 and AIP Publishing © 2013)

development of DSIF toolpath strategies and the evaluation of deformation mechanics. As a variant of DSIF, ADSIF shows distinctive characteristics in forming accuracy and deformation mechanics. This review presents an overview of the current state of the art and the most important areas of DSIF focused research as summarized.

6.1 Formability. The DSIF process exhibits a better formability than the SPIF process. The additional supporting force stabilizes local deformation and homogenizes the thickness distribution of the formed part. In terms of stress analysis, the sudden drop of stress triaxiality indicates that the possibility of failure in DSIF is lower than that in SPIF when forming the same parts. However, the unpredicted material thinning could lead to the loss of contact of the support tool with the workpiece and degenerate DSIF into a SPIF process. Thus, the avoidance of losing contact is an important prerequisite to maintain the formability of DSIF.

The maximum achievable wall angle α_{max} can be used to describe the formability of the DISF process. Similar to other ISF processes, the thickness reduction results in failure and prevents the part from achieving larger wall angles. Other indicators such as stress triaxiality are introduced from previous ISF research in terms of stress analysis and fracture evaluation. In DSIF, the wall thickness is also controlled by the squeeze factor s, which indicates the extent of the squeezing between the tools and workpiece. The squeezing effect controlled by the supporting force affects the shear and compression and is a main affecting factor to the formability in both DSIF and ADSIF. The squeezing effect improves the formability, although excessive contact pressure over deforms the workpiece and reduces the formability. The formability in DSIF is also studied by varying tool gaps and relative angles of the master and support tools. In general, the DSIF process formability is mainly dependent on the relative position between tools including the distance and angle. Alternatively, the interaction between tools can also be presented by the value of supporting force and relative position of tools.

The performance of DSIF in composite materials and high-performance alloys is investigated in the preliminary stage. For polymers, the formability improvement of DISF is confirmed as effective. For hard-to-form materials such as titanium alloys, local heating can improve the formability of the material. In the DSIF process, electric currents can be applied through the sheet and two forming tools, which provide an effective means for electrically assisted heating over SPIF processes.

6.2 Toolpath Strategies in DSIF. The toolpath strategies of DSIF can be achieved via the ADSIF, close-loop iteration, compensation, and geometrical feature-based methods. The ADSIF process is based on an in-to-out toolpath strategy that forms the workpiece from the inner annulus traveling outward to the fringe and can maintain the contact between the tools and workpiece throughout the process. This leads to improved forming accuracy and formability. The drawbacks of ADSIF include limited forming wall angle, long forming time due to the small incremental depth, and high compressive pressure throughout the process. Unlike the other toolpath strategies, reversing the forming direction also causes the change of the deformation mechanisms, which requires more in-depth investigation.

The compensation-based strategy can be divided into the prediction of tool or sheet deflections, which forms the basis for developing corresponding compensation strategies to toolpath generation. The performance of compensation-based toolpath is highly dependent on the accuracy of the prediction of forming forces and geometrical deviation as well as the algorithm of calculating the adjustment to the toolpath. The compensation-based strategy can significantly improve the forming accuracy. However, the prediction through FE simulation and experimental test is either a computing intensive process or requires iterative forming test and measurement steps.

Feature-based toolpath implements an algorithm to recognize the geometric features and adjust the density of toolpath contours. The feature recognition can be also used to improve the quality and efficiency of deflection prediction in the compensation-based strategy. In this case, the correct feature partition and the order of the forming sequence for features are of significance.

6.3 Deformation Mechanisms in DSIF. The deformation mode of DSIF is generally a combination of stretching in the meridional direction, compression in the radial direction, and slight through-thickness shear in the tool movement direction. Compared with the SPIF process, the additional support tool provides an extra compressive effect, which reduces through-thickness shear in the tool-moving direction.

The drop of stress triaxiality postpones the fracture in the double-contacted area in the DSIF process. Thus, the material failure is more likely to occur in the deformed region, starting from the outer side of the sheet and propagating in the circumferential direction due to material thinning and tool movement. In the E-DSIF process, the increase of material ductility by local heating in the contact area is another factor to defer fracture.

The deformation mechanisms in ADSIF are mainly associated with local bending of the sheet around the contact point between the workpiece and the master tool, accompanied with a squeezing effect due to the support tool as well as shearing perpendicular and parallel to the tool moving direction. The history of equivalent strain shows that there is a constant strain discrepancy between the inner and outer surfaces in ADSIF instead of the artificial dynamic oscillations and uncontrolled nature of deformation in SPIF.

In contrast to DSIF, ADSIF has high through-thickness shear and low downward pressure, as well as material bunching that counteracts the downward deformation of the sheet.

7 Recommendation for Future Work

- The improvement of accuracy and formability is still a priority in DSIF research. The combination of feature-based and compensation strategy significantly improves the forming accuracy and has the potential for further enhancement. The closed-loop algorithms allow the adjustment during the forming process based on data obtained from sensors of forming forces and potentially tool positions. For example, a pneumatic-supported support tool with an adjustable supporting force can be used to prevent loss of contact throughout the process and to provide precise control of local stress state of sheet deformation. This means it is possible to design specific DSIF toolpath either aiming for improved formability or geometrical accuracy or the combination of both.
- In terms of ADSIF, there is a need for quantitative evaluation of the forming limit. It would be useful to test the capability of forming components with wall angles over 60 deg in the ADSIF process.
- New indicators to formability, such as forming limit diagrams, can be introduced from previous ISF research since the stress triaxiality has been adapted to the DSIF process.
- FE simulation is still a powerful tool to investigate the deformation mechanics of the DSIF process accompanying with challenges. Reduction of computing time with sufficient accuracy by using adaptive mesh strategy would be beneficial to the detailed understanding of DSIF deformation mechanisms. There is a lack of work on the fracture prediction for both DSIF and ADSIF processes. Considering the material deformation under DSIF, the damage models modified with through-thickness shear may be able to predict the fracture occurrence precisely.
- In terms of deformation mechanisms, the transition of deformation modes due to the change of the squeezing factor and forming wall angle may be a research focus. Fracture in DSIF processing is assumed as stretching and tearing starting from the outer surface. However, there is a lack of established failure theory to DSIF and ADSIF process without loss of contact.
- The forming forces and thickness distribution are important in ISF research. There is a necessity to look into the effect of the squeezing between the tools and workpiece on the deflection of tools. The excessive deflection of the master tool may not only cause the geometrical inaccuracy, but also the rotation of the relative position between the master and support tools, which could lead to the change of local deformation mode. The large forming force encounters a problem with the rigidity of the DSIF machine. The design of a DSIF machine in terms of controllability and stiffness needs to be investigated.
- Electric-assisted DSIF has great potential to expend the range of sheet materials and can be implemented in the DSIF process for such as titanium alloys, or composite materials. However, the current local heating method (Fig. 8) faces problem of insulation. A possible solution is to isolate direct resistance heating on both tools to provide a local heating effect. The feasibility and efficiency of this scheme require verification by experimental testing. The capability and performance of using non-metal material, i.e., polyether ether ketone (PEEK) material in heat-assisted DSIF process are waiting for detailed assessment. The difference between the mechanics of formability improvement, such as compressive effect for metal workpiece or heating effect to void generation for polymers, can be a focus of future investigation.
- Although it is a less researched area in SPIF, design rules for DSIF toolpath generation with the consideration of process parameters and tool dimensions and arrangements could have a positive impact to not only fundamental understanding but also practical implementation of DSIF. Specific areas of interest include the toolpath design in the transition area, i.e., the sheet bending at the beginning of the forming process and the effect of tool parameter, e.g., tool radius and relative position to workpiece deformation and fracture under DSIF conditions.

Acknowledgment

This work was supported by the Engineering and Physical Sciences Research Council (grant number EP/L02084X/1).

Nomenclature

d = current thickness of the squeezed wall
s = squeeze factor—the ratio between the practical and desired tool gap
D = forming depth
t_f = the desired thickness of the formed part
t_0 = the initial thickness of the work piece
ADSIF = accumulative double-sided incremental forming
ASIF = asymmetric incremental sheet forming
BUT = bending under tension
DOST = drop of stress triaxiality
DSIF = double-sided incremental forming
FE = finite element
FLC = forming limit curve
FLD = forming limit diagram
GFLD = generalized forming limit diagram
ISF = incremental sheet forming
MaxR = the outer radius of the desired forming truncated cone
PEEK = polyether ether ketone
SPIF = single-point incremental forming
Step depth/Δz = the distance the tool moves down after completing an entire closed loop in toolpath
TPIF = two-point incremental forming
α = wall angle

References

[1] Emmens, W. C., Sebastiani, G., and van den Boogaard, A. H., 2010, "The Technology of Incremental Sheet Forming—A Brief Review of the History," J. Mater. Process. Technol., **210**(8), pp. 981–997.
[2] Mason, B., and Applton, E., 1984, "Sheet Metal Forming for Small Batches Using Sacrificial Tooling," 3rd International Conference on Rotary Metalworking Processes (ROMP 3), Kyoto, Japan, Sept.
[3] Silva, M. B., and Martins, P. A. F., 2012, "Two-Point Incremental Forming With Partial Die: Theory and Experimentation," J. Mater. Eng. Perform., **22**(4), pp. 1018–1027.
[4] Hirt, G., Bambach, M., Bleck, W., Prahl, U., and Stollenwerk, J., 2015, "The Development of Incremental Sheet Forming From Flexible Forming to Fully Integrated Production of Sheet Metal Parts," Advances in Production Technology, Springer, New York, pp. 117–129.
[5] Maidagan, E., Zettler, J., Bambach, M., Rodríguez, P. P., and Hirt, G., 2007, "A New Incremental Sheet Forming Process Based on a Flexible Supporting Die System," Key Eng. Mater., **344**, pp. 607–614.
[6] Meier, H., Smukala, V., Dewald, O., and Zhang, J., 2007, "Two Point Incremental Forming With Two Moving Forming Tools," Key Eng. Mater., **344**, pp. 599–605.
[7] Smith, J., Malhotra, R., Liu, W. K., and Cao, J., 2013, "Deformation Mechanics in Single-Point and Accumulative Double-Sided Incremental Forming," Int. J. Adv. Manuf. Technol., **69**(5–8), pp. 1185–1201.
[8] Hagan, E., and Jeswiet, J., 2003, "A Review of Conventional and Modern Single-Point Sheet Metal Forming Methods," Proc. Inst. Mech. Eng., Part B, **217**(2), pp. 213–225.
[9] Micari, F., Ambrogio, G., and Filice, L., 2007, "Shape and Dimensional Accuracy in Single Point Incremental Forming: State of the art and Future Trends," J. Mater. Process. Technol., **191**(1–3), pp. 390–395.
[10] Emmens, W. C., and van den Boogaard, A. H., 2009, "Incremental Forming by Continuous Bending under Tension—An Experimental Investigation," J. Mater. Process. Technol., **209**(14), pp. 5456–5463.
[11] Duflou, J. R., Habraken, A.-M., Cao, J., Malhotra, R., Bambach, M., Adams, D., Vanhove, H., Mohammadi, A., and Jeswiet, J., 2018, "Single Point Incremental Forming: State-of-the-Art and Prospects," Int. J. Mater. Form. **11**(6), pp. 743–773.
[12] Gatea, S., Ou, H. G., and McCartney, G., 2016, "Review on the Influence of Process Parameters in Incremental Sheet Forming," Int. J. Adv. Manuf. Technol., **87**(1–4), pp. 479–499.

[13] Behera, A. K., de Sousa, R. A., Ingarao, G., and Oleksik, V., 2017, "Single Point Incremental Forming: An Assessment of the Progress and Technology Trends From 2005 to 2015," J. Manuf. Process., **27**, pp. 37–62.
[14] Jeswiet, J., Micari, F., Hirt, G., Bramley, A., Duflou, J., and Allwood, J., 2005, "Asymmetric Single Point Incremental Forming of Sheet Metal," CIRP Ann., **54**(2), pp. 88–114.
[15] Afonso, D., Alves de Sousa, R., and Torcato, R., 2017, "Integration of Design Rules and Process Modelling Within SPIF Technology—A Review on the Industrial Dissemination of Single Point Incremental Forming," Int. J. Adv. Manuf. Technol., **94**(9–12), pp. 4387–4399.
[16] Fang, Y., Lu, B., Chen, J., Xu, D. K., and Ou, H., 2014, "Analytical and Experimental Investigations on Deformation Mechanism and Fracture Behavior in Single Point Incremental Forming," J. Mater. Process. Technol., **214**(8), pp. 1503–1515.
[17] Yamashita, M., Gotoh, M., and Atsumi, S.-Y., 2008, "Numerical Simulation of Incremental Forming of Sheet Metal," J. Mater. Process. Technol., **199**(1–3), pp. 163–172.
[18] Lu, B., Chen, J., Ou, H., and Cao, J., 2013, "Feature-Based Tool Path Generation Approach for Incremental Sheet Forming Process," J. Mater. Process. Technol., **213**(7), pp. 1221–1233.
[19] Allwood, J. M., Music, O., Raithathna, A., and Duncan, S. R., 2009, "Closed-Loop Feedback Control of Product Properties in Flexible Metal Forming Processes With Mobile Tools," CIRP Ann., **58**(1), pp. 287–290.
[20] Azaouzi, M., and Lebaal, N., 2012, "Tool Path Optimization for Single Point Incremental Sheet Forming Using Response Surface Method," Simul. Model. Pract. Theory, **24**, pp. 49–58.
[21] Matsubara, S., 2001, "A Computer Numerically Controlled Dieless Incremental Forming of a Sheet Metal," Proc. Inst. Mech. Eng., Part B, **215**(7), pp. 959–966.
[22] Hirt, G., Ames, J., and Bambach, M., 2006, "Basic Investigation Into the Characteristics of Dies and Support Tools Used in CNC-Incremental Sheet Forming," Proceedings of the International Deep Drawing Research Group Conference, Leca do Balio, Portugal, June 19–21.
[23] Malhotra, R., Cao, J., Ren, F., Kiridena, V., Cedric Xia, Z., and Reddy, N. V., 2011, "Improvement of Geometric Accuracy in Incremental Forming by Using a Squeezing Toolpath Strategy With Two Forming Tools," ASME J. Manuf. Sci. Eng., **133**(6), p. 061019.
[24] Malhotra, R., Cao, J., Beltran, M., Xu, D., Magargee, J., Kiridena, V., and Xia, Z. C., 2012, "Accumulative-DSIF Strategy for Enhancing Process Capabilities in Incremental Forming," CIRP Ann., **61**(1), pp. 251–254.
[25] Lasunon, O., and Knight, W. A., 2007, "Comparative Investigation of Single-Point and Double-Point Incremental Sheet Metal Forming Processes," Proc. Inst. Mech. Eng., Part B, **221**(12), pp. 1725–1732.
[26] Wu, J. H., and Wang, Q. C., 2014, "Comparison of the Geometric Accuracy by DSIF Toolpath With SPIF Toolpath," Appl. Mech. Mater., **494–495**, pp. 497–501.
[27] Sortais, H. C., Kobayashi, S., and Thomsen, E., 1962, *Mechanics of Conventional Spinning*, University of California, Berkeley.
[28] Ren, H., Moser, N., Zhang, Z., Ndip-Agbor, E., Smith, J., Ehmann, K. F., and Cao, J., 2015, "Effects of Tool Positions in Accumulated Double-Sided Incremental Forming on Part Geometry," ASME J. Manuf. Sci. Eng., **137**(5), p. 051008.
[29] Ndip-Agbor, E., Smith, J., Ren, H., Jiang, Z., Xu, J., Moser, N., Chen, W., Xia, Z. C., and Cao, J., 2015, "Optimization of Relative Tool Position in Accumulative Double Sided Incremental Forming Using Finite Element Analysis and Model Bias Correction," Int. J. Mater. Form., **9**(3), pp. 371–382.
[30] Lu, B., Fang, Y., Xu, D. K., Chen, J., Ai, S., Long, H., Ou, H., and Cao, J., 2015, "Investigation of Material Deformation Mechanism in Double Side Incremental Sheet Forming," Int. J. Mach. Tools Manuf., **93**, pp. 37–48.
[31] Allwood, J. M., and Shouler, D. R., 2009, "Generalised Forming Limit Diagrams Showing Increased Forming Limits With Non-Planar Stress States," Int. J. Plast., **25**(7), pp. 1207–1230.
[32] Lu, B., Xu, D. K., Liu, R. Z., Ou, H., Long, H., Chen, J., 2015, "Cranial Reconstruction Using Double Side Incremental Forming," Key Eng. Mater., **639**, pp. 535–542.
[33] Davarpanah, M. A., Mirkouei, A., Yu, X., Malhotra, R., and Pilla, S., 2015, "Effects of Incremental Depth and Tool Rotation on Failure Modes and Microstructural Properties in Single Point Incremental Forming of Polymers," J. Mater. Process. Technol., **222**, pp. 287–300.
[34] Davarpanah, M. A., and Malhotra, R., 2018, "Formability and Failure Modes in Single Point Incremental Forming of Metal-Polymer Laminates," Procedia Manuf., **26**, pp. 343–348.
[35] Jackson, K. P., Allwood, J. M., and Landert, M., 2008, "Incremental Forming of Sandwich Panels," J. Mater. Process. Technol., **204**(1–3), pp. 290–303.
[36] Fiorotto, M., Sorgente, M., and Lucchetta, G., 2010, "Preliminary Studies on Single Point Incremental Forming for Composite Materials," Int. J. Mater. Form., **3**(S1), pp. 951–954.
[37] Davarpanah, M. A., Zhang, Z., Bansal, S., Cao, J., and Malhotra, R., 2016, "Preliminary Investigations on Double Sided Incremental Forming of Thermoplastics," Manuf. Lett., **8**, pp. 21–26.
[38] Ji, Y. H., and Park, J. J., 2008, "Formability of Magnesium AZ31 Sheet in the Incremental Forming at Warm Temperature," J. Mater. Process. Technol., **201**(1–3), pp. 354–358.
[39] Ambrogio, G., Filice, L., and Manco, G. L., 2008, "Warm Incremental Forming of Magnesium Alloy AZ31," CIRP Ann., **57**(1), pp. 257–260.
[40] Duflou, J. R., Callebaut, B., Verbert, J., and De Baerdemaeker, H., 2007, "Laser Assisted Incremental Forming: Formability and Accuracy Improvement," CIRP Ann., **56**(1), pp. 273–276.
[41] Otsu, M., Yasunaga, M., Matsuda, M., and Takashima, K., 2014, "Friction Stir Incremental Forming of A2017 Aluminum Sheets," Procedia Eng., **81**, pp. 2318–2323.
[42] Xu, D., Wu, W., Malhotra, R., Chen, J., Lu, B., and Cao, J., 2013, "Mechanism Investigation for the Influence of Tool Rotation and Laser Surface Texturing (LST) on Formability in Single Point Incremental Forming," Int. J. Mach. Tools Manuf., **73**, pp. 37–46.
[43] Göttmann, A., Bailly, D., Bergweiler, G., Bambach, M., Stollenwerk, J., Hirt, G., and Loosen, P., 2012, "A Novel Approach for Temperature Control in ISF Supported by Laser and Resistance Heating," Int. J. Adv. Manuf. Technol., **67**(9–12), pp. 2195–2205.
[44] Palumbo, G., and Brandizzi, M., 2012, "Experimental Investigations on the Single Point Incremental Forming of a Titanium Alloy Component Combining Static Heating With High Tool Rotation Speed," Mater. Des., **40**, pp. 43–51.
[45] Xu, D. K., Lu, B., Cao, T. T., Zhang, H., Chen, J., Long, H., and Cao, J., 2016, "Enhancement of Process Capabilities in Electrically-Assisted Double Sided Incremental Forming," Mater. Des., **92**, pp. 268–280.
[46] Valoppi, B., Sánchez Egea, A. J., Zhang, Z., González Rojas, H. A., Ghiotti, A., Bruschi, S., and Cao, J., 2016, "A Hybrid Mixed Double-Sided Incremental Forming Method for Forming Ti6Al4V Alloy," CIRP Ann., **65**(1), pp. 309–312.
[47] Zhang, Z. X., Ren, H. Q., Xu, R., Moser, N., Smith, J., Ndip-Agbor, E., Malhotra, R., Xia, Z. C., Ehmann, K. F., and Cao, J., 2015, "A Mixed Double-Sided Incremental Forming Toolpath Strategy for Improved Geometric Accuracy," ASME J. Manuf. Sci. Eng., **137**(5), p. 051007.
[48] Moser, N., Pritchet, D., Ren, H., Ehmann, K. F., and Cao, J., 2016, "An Efficient and General Finite Element Model for Double-Sided Incremental Forming," ASME J. Manuf. Sci. Eng., **138**(9), p. 091007.
[49] Meier, H., Buff, B., Laurischkat, R., and Smukala, V., 2009, "Increasing the Part Accuracy in Dieless Robot-Based Incremental Sheet Metal Forming," CIRP Ann., **58**(1), pp. 233–238.
[50] Rakesh, L., Amit, S., and Reddy, N. V., 2016, "Deflection Compensations for Tool Path to Enhance Accuracy During Double-Sided Incremental Forming," ASME J. Manuf. Sci. Eng., **138**(9), p. 091008.
[51] Ren, H., Li, F., Moser, N., Leem, D., Li, T., Ehmann, K., and Cao, J., 2018, "General Contact Force Control Algorithm in Double-Sided Incremental Forming," CIRP Ann., **67**(1), pp. 381–384.
[52] Wang, H., Zhang, R., Zhang, H., Hu, Q., and Chen, J., 2018, "Novel Strategies to Reduce the Springback for Double-Sided Incremental Forming," Int. J. Adv. Manuf. Technol., **96**(1–4), pp. 973–979.
[53] Meier, H., Magnus, C., and Smukala, V., 2011, "Impact of Superimposed Pressure on Dieless Incremental Sheet Metal Forming With Two Moving Tools," CIRP Ann., **60**(1), pp. 327–330.
[54] Malhotra, R., Reddy, N., and Cao, J., 2010, "Automatic 3D Spiral Toolpath Generation for Single Point Incremental Forming," ASME J. Manuf. Sci. Eng., **132**(6), p. 061003.
[55] Lingam, R., Prakash, O., Belk, J. H., and Reddy, N. V., 2016, "Automatic Feature Recognition and Tool Path Strategies for Enhancing Accuracy in Double Sided Incremental Forming," Int. J. Adv. Manuf. Technol., **88**(5–8), pp. 1639–1655.
[56] Ndip-Agbor, E., Ehmann, K., and Cao, J., 2017, "Automated Flexible Forming Strategy for Geometries With Multiple Features in Double-Sided Incremental Forming," ASME J. Manuf. Sci. Eng., **140**(3), p. 031004.
[57] Moser, N., Zhang, Z., Ren, H., Zhang, H., Shi, Y., Ndip-Agbor, E. E., Lu, B., Chen, J., Ehmann, K. F., and Cao, J., 2016, "Effective Forming Strategy for Double-Sided Incremental Forming Considering In-Plane Curvature and Tool Direction," CIRP Ann., **65**(1), pp. 265–268.
[58] Martins, P. A. F., Bay, N., Skjoedt, M., and Silva, M. B., 2008, "Theory of Single Point Incremental Forming," CIRP Ann., **57**(1), pp. 247–252.
[59] Lu, B., Fang, Y., Xu, D. K., Chen, J., Ou, H., Moser, N. H., and Cao, J., 2014, "Mechanism Investigation of Friction-Related Effects in Single Point Incremental Forming Using a Developed Oblique Roller-Ball Tool," Int. J. Mach. Tools Manuf., **85**, pp. 14–29.
[60] Eyckens, P., Belkassem, B., Henrard, C., Gu, J., Sol, H., Habraken, A. M., Duflou, J. R., Van Bael, A., and Van Houtte, P., 2011, "Strain Evolution in the Single Point Incremental Forming Process: Digital Image Correlation Measurement and Finite Element Prediction," Int. J. Mater. Form., **4**(1), pp. 55–71.
[61] Malhotra, R., Xue, L., Belytschko, T., and Cao, J., 2012, "Mechanics of Fracture in Single Point Incremental Forming," J. Mater. Process. Technol., **212**(7), pp. 1573–1590.
[62] Gatea, S., Ou, H. G., Lu, B., and McCartney, G., 2017, "Modelling of Ductile Fracture in Single Point Incremental Forming Using a Modified GTN Model," Eng. Fract. Mech., **186**, pp. 59–79.
[63] Gatea, S., Xu, D., Ou, H., and McCartney, G., 2017, "Evaluation of Formability and Fracture of Pure Titanium in Incremental Sheet Forming," Int. J. Adv. Manuf. Technol., **95**(1–4), pp. 625–641.
[64] Wang, C., Daniel, W. J. T., Lu, H., Liu, S., and Meehan, P. A., 2017, "FEM Investigation of Ductile Fracture Prediction in Two-Point Incremental Sheet Metal Forming Process," International Conference on the Technology of Plasticity, Procedia Engineering, Cambridge, UK, Sept. 17–22, Vol 207, pp. 836–841.
[65] Valoppi, B., Zhang, Z., Deng, M., Ghiotti, A., Bruschi, S., Ehmann, K. F., and Cao, J., 2017, "On the Fracture Characterization in Double-Sided Incremental Forming of Ti6Al4 V Sheets at Elevated Temperatures," Procedia Manuf., **10**, pp. 407–416.
[66] Ndip-Agbor, E. E., Smith, J., Xu, R., Malhotra, R., and Cao, J., 2013, "Effect of Relative Tool Position on the Geometric Accuracy of Accumulative DSIF," AIP Conf. Proc., **1567**(1), pp. 828–831.